Heliyon 10 (2024) e26916

Contents lists available at ScienceDirect

Heliyon

journal homepage: www.cell.com/heliyon

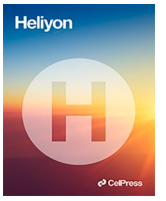

Research article

Integrated network pharmacology and phosphoproteomic analyses of Baichanting in Parkinson's disease model mice

Xin Gao [a], Jiaqi Fu [a], DongHua Yu [b], Fang Lu [b], Shumin Liu [b,*]

[a] Heilongjiang University of Chinese Medicine, College of Pharmacy, Harbin, 150040, China
[b] Heilongjiang University of Chinese Medicine, Research Institute of Chinese Medicine, Harbin, 150040, China

ARTICLE INFO

Keywords:
Parkinson's disease
Baichanting compound
Apoptosis
Phosphorylation

ABSTRACT

The incidence rate of Parkinson's disease (PD) is increasing yearly. Neuronal apoptosis caused by abnormal protein phosphorylation is closely related to the pathogenesis of Parkinson's disease. At present, few PD-specific apoptosis pathways have been revealed. To investigate the effect of Baichanting (BCT) on apoptosis from the perspective of protein phosphorylation, α-syn transgenic mice were selected to observe the behavioral changes of the mice, and the apoptosis of substantia nigra cells were detected by the HE method and TUNEL method. Network pharmacology combined with phosphorylation proteomics was used to find relevant targets for BCT treatment of PD and was further verified by PRM and western blotting. BCT improved the morphology of neurons in the substantia nigra and reduced neuronal apoptosis. The main enriched pathways in the network pharmacology results were apoptosis, the p53 signaling pathway and autophagy. Western blot results showed that BCT significantly regulated the protein expression levels of BAX, Caspase-3, LC3B, P53 and mTOR and upregulated autophagy to alleviate apoptosis. Using phosphorylated proteomics and PRM validation, we found that Pak5, Grin2b, Scn1a, BcaN, L1cam and Braf are closely correlated with the targets of the web-based pharmacological screen and may be involved in p53/mTOR-mediated autophagy and apoptosis pathways. BCT can inhibit the activation of the p53/mTOR signaling pathway, thereby enhancing the autophagy function of cells, and reducing the apoptosis of neurons which is the main mechanism of its neuroprotective effect.

1. Introduction

Parkinson's disease (PD) is the second most common neurodegenerative disease worldwide, with resting tremor, bradykinesia and muscle stiffness as frequent symptoms [1]. A variety of nonmotor symptoms are also common in Parkinson's disease, including smell disorders, sleep disorders, lipid metabolism disorders, dementia, and depression [2–4].The pathogenesis of Parkinson's disease is complex and is based on the degeneration and loss of dopaminergic neurons in the substantia nigra and the protein aggregation of α-synuclein(α-syn) in the cytoplasm of the remaining neurons in the substantia nigra [5]. Under physiological conditions, α-syn can maintain the function of synapses and can be involved in regulating dopamine biosynthesis [6]. Environmental or genetic changes can easily lead to the misfolding of α-syn, the emergence of oligomers, the gradual increase in fibrous proteins, the emergence of Lewy bodies, and finally the programmed death of dopaminergic nerve cells, resulting in PD symptoms in patients [7,8]. Protein

* Corresponding author.
E-mail address: shumliu0321@163.com (S. Liu).

https://doi.org/10.1016/j.heliyon.2024.e26916
Received 13 June 2023; Received in revised form 21 February 2024; Accepted 21 February 2024
Available online 27 February 2024

phosphorylation refers to the process of transferring ATP phosphate groups to protein amino acid residues (serine, threonine, tyrosine) catalyzed by protein kinase or binding GTP under signal action. It is a universal regulatory mode in organisms and plays an important role in the process of cell signal transduction [9]. It has been a research hotspot of PD molecular pathogenesis in recent decades. Modern research has found that the occurrence and development of PD is related to the imbalance between autophagy and apoptosis caused by abnormal protein phosphorylation [10]. In some cases, autophagy inhibits apoptosis and is a survival pathway of cells, but autophagy and apoptosis also work together to induce cell death, and the two pathways are interrelated and regulate each other [11]. According to a report, the HE team found that the autophagy pathway in the substantia nigra of Parkinson's disease model mice was severely inhibited, which was caused by Cdk5 protein promoting abnormal phosphorylation of Ank2 protein and activating the p25/Cdk2 pathway [12]. When the phosphorylation degree of the IGF1R/PI3K/AKT cell survival signaling pathway is enhanced, the apoptosis of substantia nigra cells in the brain is weakened, which can alleviate the symptoms of Parkinson's disease [13]. However, the mechanism and pathological pathway remain unclear. Although various potential phosphorylation pathways from clinical, neuroimaging and biochemical studies have been proposed, the specific and reliable biological pathway of PD is still elusive. On the other hand, there is no effective treatment method for the disease, and commonly used clinical drugs(statins, benzodiazepines, metformin, etc.) are prohibitive for patients due to their severe adverse reactions such as hypotension and involuntary movements [14–17]. Therefore, exploring new therapeutic drugs has become an urgent problem to be solved.

From the point of view of Chinese medicine, PD falls within the category of "shaking syndrome". Among them, deficiency of the liver and kidney is the root of the disease. Therefore, the treatment focuses on "nourishing the liver and kidney, and calming the liver and suppressing wind" for principle [18]. The BCT studied in this paper is refined from Fuyuanpingchanning compound, an experienced prescription for clinical treatment of PD, and is a combination of Acanthopanax senticosus, Paeonia lactiflora and Uncaria chinensis [19]. Among them, Acanthopanax senticosus is good for nourishing Qi and kidney, and white Paeonia lactiflora can nourish blood and soften liver. Uncaria can clear heat and calm the liver. The compound formula composed of three herbs can nourish the liver and kidney, nourish Qi and blood, and treat PD from the source of the disease. Previous research by the research group found that Baichanting Compound can regulate apoptosis by reducing the content of various inflammatory factors and NO in the substantia nigra and regulating the level of oxidative stress factors, thus playing a neuroprotective role. However, it was found through data review that many inflammatory factors and oxidative stress factors have physiological effects through phosphorylation [20,21]. Therefore, it makes sense to study whether the neuroprotective effect of BCT is related to the intervention of protein phosphorylation to regulate autophagy and apoptosis.

In the current project, we used network pharmacology to predict "Chinese medicine-components-target-pathway" to narrow the scope and clarify the direction of phosphorylation analysis in subsequent experiments. Animal behavior experiments were used to study the effect of BCT on the motor coordination of the model, and histopathological observations were made on the substantia nigra of mice to evaluate the pathological changes in the central nervous system of the model induced by BCT. Based on western blotting and protein phosphorylation techniques, the mechanism by which BCT regulates apoptosis in the treatment of PD by regulating the phosphorylation pathway was clarified.

2. Materials and methods

2.1. Chemicals and reagents

Medicinal herbs: The Chinese herbal medicine used in this study included Acanthopanax senticosus (Rupr. Maxim.) harms (purchased from Wuchang County, Heilongjiang Province, with a growth period of six years), Cynanchum otophylum (purchased from Haozhou City, Anhui Province), and Uncaria rhynchophylla (Miq.) Miq. ex Havil (purchased from Jianhe County, Guizhou Province). The TUNEL kit (Jiancheng), BCA protein concentration assay kit (Solarbio), RIPA lysis buffer (Solarbio), 5 × protein loading buffer (Biosntech), SDS−PAGE gel preparation kit (Biosharp), Tris Base (Sigma), sodium dodecyl sulfate (Nachuan), special nonfat milk powder for sealing (Pulilai Gene), Tween 20 (BIOFROXX), western secondary antibody removal solution (Beyotime), hypersensitive ECL luminescent liquid (Meilunbio), LC3B (Sanying), P53 (Abcam), AMPK (Abcam), mTOR (Abcam), BAX (Boaosen), Caspase-3 (Boaosen), GAPDH (Boaosen), protease inhibitor (Calbiochem), pancreatin (Promega), acetonitrile (Fisher Chemical), trifluoroacetic acid (Sigma Aldrich), formic acid (FLUKA), iodoacetamide (Sigma), dithiothreitol (Sigma), urea (Sigma), triethylammonium bicarbonate (Sigma), purified water (Fisher Chemical), BCA Kit (Biyuntian), TMT labeling kit (Thermo), and phosphorylase inhibitor (Millipore) were the chemicals used in our study.

2.2. BCT preparation

According to the prescribed ratio of Acanthopanax senticosus extract: peony extract: Uncaria extract = 54.0:45.0:82.5, Acanthopanax senticosus and Cynanchum otophylum were extracted by refluxing with 70% ethanol and were then concentrated and freeze-dried. Similarly, Uncaria rhynchophylla was extracted using 80% ethanol reflux and was then concentrated and freeze-dried. Each of the above extracts was prepared by dissolving an appropriate amount of the lyophilized powder in 0.5% CMC-Na aqueous solution.

2.3. Animal treatment

Ten-month-old male alpha-synuclein(A53T) transgenic mice(B6; C3-Tg(Prnp-SNCA*A53T)83Vle/J) and matched male wild-type C57BL/6J mice were included in the study(weighing 20–30 g). The mice were provided by JICUIYAOKAN Biotechnology Co., Ltd.

The room temperature was maintained at 22 °C, and the relative humidity was 65 ± 5%. The mice were provided access to food and water. The protocol was approved by the Committee on the Ethics of Animal Experiments of Heilongjiang University of Chinese Medicine, China, and the approval number was 2022072102.

After acclimatization, the mice were randomly divided into five groups(n = 8):normal control group(C57BL/6J mice), model group (α-syn mice), low-dose group(α-syn + BCT 95.75 mg/kg), middle-dose group(α-syn + BCT 181.5 mg/kg), high-dose group(α-syn + BCT 363 mg/kg). The α-syn + BCT group was intraperitoneally gavaged with BCT daily for 21 days. The NC and model groups were administered saline (20 ml/kg daily).

After administration,the brain tissue of the mice was eviscerated and placed on ice. The striatum was stripped, weighed, and stored in liquid nitrogen until further use. Later, the sample was kept on ice and ground quickly using a glass homogenizer to prepare a suspension, which was centrifuged at 15,000 r/min for 15 min at 4 °C. The supernatant was used as the test solution.

2.4. Network pharmacology

The components of BCT were imported into the TCMSP and Taiwan Traditional Chinese Medicine Database to search for action targets, and the components were selected with OB ≥ 30 and DL ≥ 0.18 as screening conditions (Tabel S1). The ingredients were imported into SwissTargetPrediction and stirred for target mapping, and the targets were imported into the UniProt database to filter out the targets of nonhumans and mice, delete duplicates, and obtain the relevant targets of TCM. The Online Mendelian Inheritance in Man (OMIM, https://omim.org/) and GeneCards (https://www.genecards.org/) gene maps were searched using the keywords "Parkinson's disease" to identify potential PD targets. The projected target of BCT against PD was thought to be the intersection of medication and disease targets. To standardize the gene and protein names, these targets were imported into UniProtKB (http://www.UniProt. org/). A protein–protein interaction (PPI) network was created using Cytoscape 3.9.0 and STRING 11.0 (https://string-db.org/). The intersection targets were imported into the Metascape database for GO and KEGG enrichment analysis.

2.5. Behavioral experiments

Pole climbing experiment: A wooden pole with a length of 100 cm was chosen, and the climbing tape was wrapped around it entirely. The mouse was placed head down on the top of the pole and allowed to climb down naturally, and the total time from standing on the top of the pole with the two hind limbs to contacting the bottom of the pole with the two front limbs was recorded.

Autonomous activity experiment: The mice were placed on the autonomous activity counterboard for 2 min, and the activity of the mice was recorded for 5 min.

2.6. Histopathology and immunohistochemistry staining

The thorax of the mouse was cut open and infused with 0.9% normal saline through the left ventricle until the fluid flowing out of the right atrium was colorless normal saline. Brains were perfused with 4% paraformaldehyde and fixed for 48 h. Gradient ethanol dehydration, xylene transparency, paraffin embedding and sectioning were performed. Paraffin sections were dewaxed with xylene and ethanol to water, stained with hematoxylin for 10 min, differentiated with 0.7% hydrochloric alcohol, and impregnated with eosin for 3 min. Gradient ethanol dehydration, xylene transparent, neutral gum seal. Immunohistochemistry: Brain tissue sections were prepared, antigens were repaired, and the sections were placed in 3% hydrogen peroxide solution to block endogenous peroxidase, and incubated with primary antibody at 4 °C overnight. Secondary antibody (HRP label) was added, incubated at room temperature for 50 min, color was developed with DAB reagent, and then hemoxylin was re-dyed and the tablets were sealed. Three fields of view were randomly selected for each sample, and images were collected at 200 times of the microscope. Images were observed and photographed under the optical microscope. Image-Pro Plus6.0 software was used to determine the area of positive expression.

2.7. Western blotting

Thirty micrograms of sample protein solution were used for sample loading, the starting voltage was set to 80 V, bromophenol blue was run onto the separation gel, and the voltage was increased to 120 V–130 V for electrophoresis for 60 min. After sample blocking, the primary and secondary antibodies were combined and incubated for 1 h at room temperature. The membrane was washed and immersed in ECL luminescent agent, protected from light for 2 min and then scanned for grayscale values.

2.8. Phosphoproteomic detection

Protein extraction, digestion, and labeling: After the samples were sufficiently ground and lysed, the protein concentration was determined using a BCA kit. Peptides were fractionated using Thermo Betasil C18 columns. The modified peptides were eluted with 10% ammonia. The eluate was lyophilized and desalted according to the instructions for the C18 zip tip. Phosphoproteomics quantitation analysis: The tryptic peptides were dissolved in solvent A (0.1% formic acid) and directly loaded onto a homemade reversed-phase analytical column (15 cm length, 75 μm I.D.). A constant flow rate of 400 nL/min was set, and an EASY-nLC 1000 UPLC system was used. The peptides were subjected to an NSI source followed by tandem mass spectrometry (MS/MS) in Q ExactiveTM Plus (Thermo) coupled to the UPLC online. The electrospray voltage was set to 2.0 kV. The *m/z* scan range was set to 350 to 1800 for a full scan, and intact peptides were detected using Orbitrap at a resolution of 70,000. Mass spectrometry quality control test: Most of the

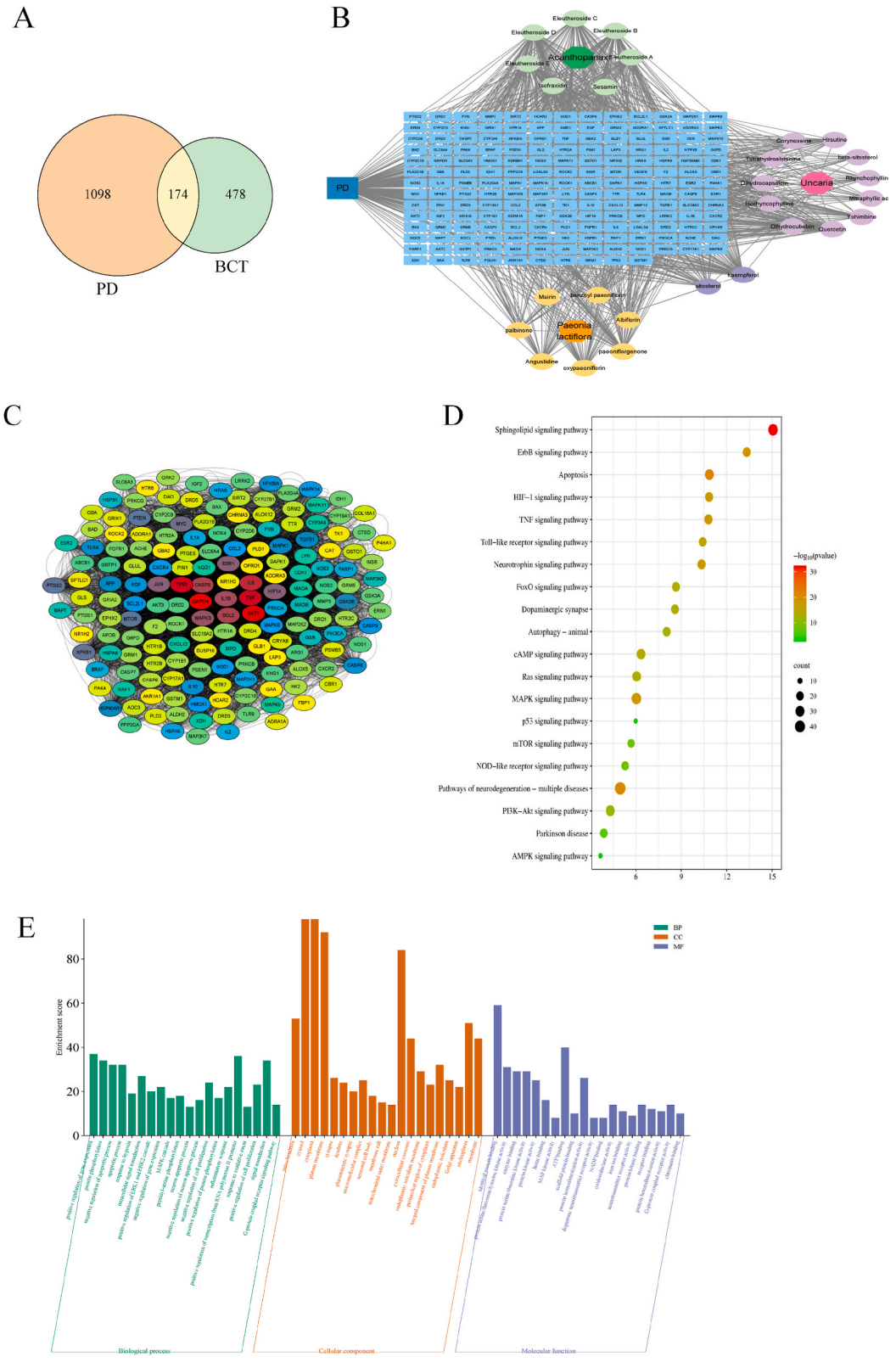

Fig. 1. Network pharmacology analysis of BCT treating PD. (A)Venn diagram of PD and BCT. (B)Disease -BCT component - target diagram. (C) The PPI network of BCT treatment on PD. Node color reflects its degree. (D) The KEGG pathways enrichment analysis. (E) The GO enrichment analysis.

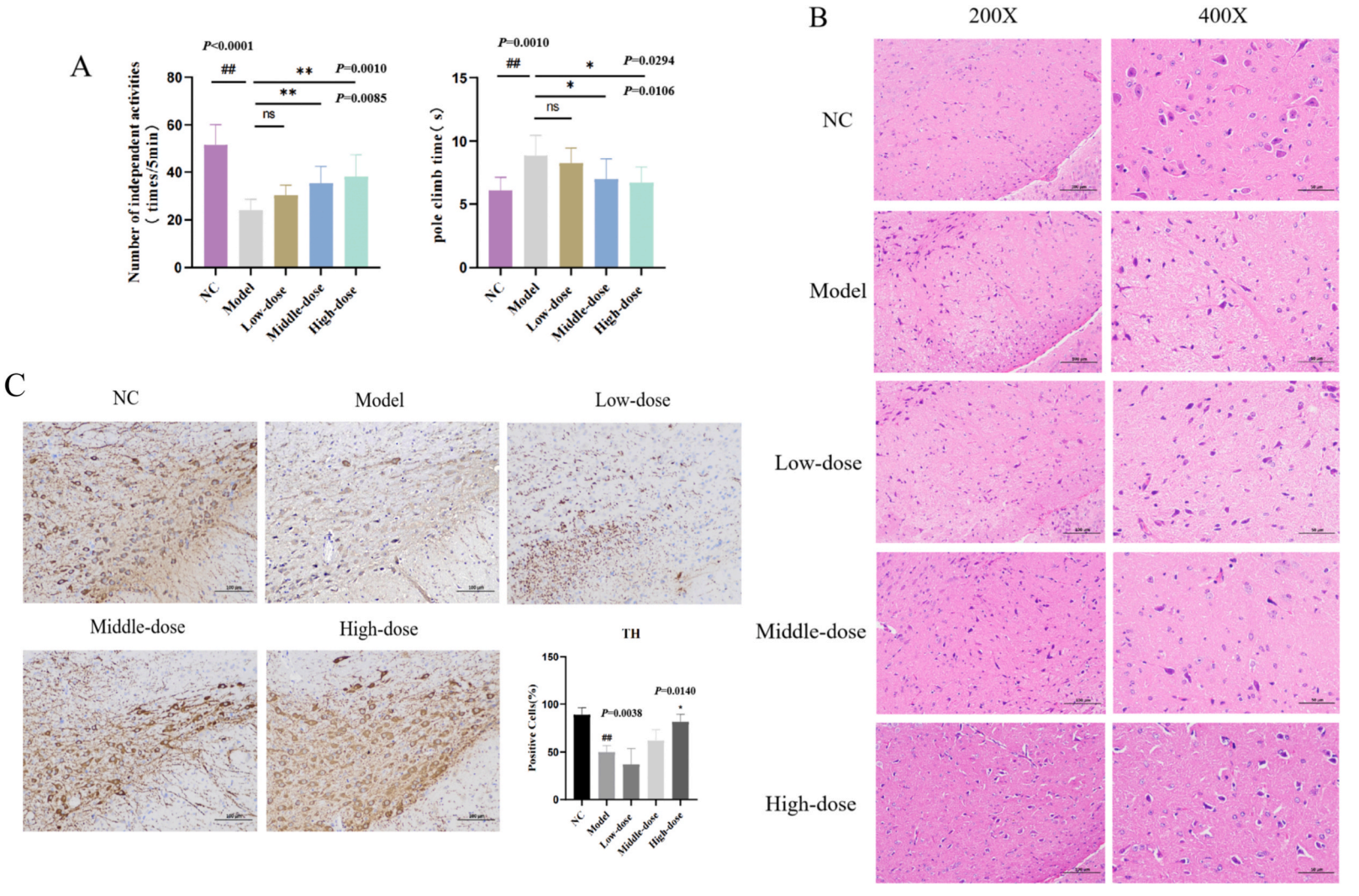

Fig. 2. (A)Behavioral experiments results evaluated the degree of motor impairment in mice. (B)HE staining represents neuronal changes in the substantia nigra region(scale bar = 100 μm). (C) Immunohistochemistry indicated Tyrosine hydroxylase-positive (TH^+) expression(scale bar = 100 μm). * Significantly different from the model group at $P < 0.05$.** Significantly different from the model group at $P < 0.01$. # Significantly different from the control group at $P < 0.05$. ## Significantly different from the control group at $P < 0.01$ (one-way ANOVA).

peptides were distributed in 7–20 amino acids, which is consistent with the rule based on the enzymatic hydrolysis of trypsin and HCD fragmentation (Fig. S1A). The distribution of peptide length identified by MS met the quality control requirements. The first-order mass error of most spectra is within 10 ppm (within 70 ppm of the timsTOF mass spectrum), which is in accordance with the high-precision characteristics of the mass spectrum (Fig. S1B).

2.9. PRM validation experiment

Protein extraction and trypsin hydrolysis: The protein concentration was determined by a BCA kit. The same amount of each sample protein was used for enzymatic hydrolysis, trypsin was added, and enzymatic hydrolysis was performed overnight. Dithiothreitol (DTT) was added to a final concentration of 5 mm and reduced at 56 °C for 30 min. Then, iodoacetamide (IAA) was added to a final concentration of 11 mm and incubated at room temperature in the dark for 15 min. Liquid chromatography–mass spectrometry: The peptide segments were dissolved by liquid chromatography mobile phase a (0.1% (V/V) formic acid aqueous solution) and separated by easy NLC 1000 ultra high-performance liquid system. Mobile phase A was an aqueous solution containing 0.1% formic acid and 2% acetonitrile; mobile phase B was an aqueous solution containing 0.1% formic acid and 90% acetonitrile. The liquid phase gradient settings were as follows: 0–40 min, 6%–25% B; 40–52 min, 25%–35% B; 52–56 min, 35%–80% B; 56–60 min, 80% B. The flow rate was maintained at 500 NL/min. After separation by an ultrahigh-performance liquid chromatography system, the peptide was injected into an NSI ion source for ionization and then analyzed by Q Exactive TM plus mass spectrometry. The ion source voltage was set to 2.1 kV, and the peptide parent ions and their secondary fragments were detected and analyzed by high-resolution Orbitrap. The scanning range of primary mass spectrometry was set to 370–1090 M/Z, and the scanning resolution was set to 70000. The scanning resolution of the secondary mass spectrometry Orbitrap was set to 17500. The data acquisition mode used a data independent scanning (DIA) program, and the fragmentation energy of the HCD collision pool was set to 27. The automatic gain control (AGC) of primary mass spectrometry was set to 3e6, and the maximum ion implantation time (it) was set to 50 ms. The automatic gain control (AGC) of secondary mass spectrometry was set to 1E5, the maximum ion implantation time (it) was set to 200 ms, and the isolation window was set to 1.6 *m/z*.

2.10. Statistical analysis

SPSS 21.0 and GraphPad Prism statistical software were used for statistical analysis. The measurement data are presented as the mean ± standard deviation. One-way analysis of variance was used for comparisons among multiple groups, and a *t*-test was used for comparisons between two groups. $P < 0.05$ was considered statistically significant.

3. Results

3.1. Network pharmacological analysis

We retrieved 1274 nonduplicated PD-related targets in the GeneCards and OMIM databases and combined 27 active components and 652 potential targets obtained from BCT with the Venn diagram constructed by the Venny website to obtain 174 intersection targets (Fig. 1A). Cytoscape 3.9.0 software was used to construct the pharmacochemical component-target network diagram to obtain possible core components of BCT for PD treatment (Fig. 1B). The common targets of BCT and disease were imported into the STRING database for protein–protein interactions((Fig. 1C). The common targets of BCT and disease were imported into the STRING database for protein–protein interaction (PPI) analysis (Fig. 2C).

All the networks were merged, and the analysis showed that the signaling pathways mainly involved axon guidance, long-term potential, dopaminergic synapses and other key targets, such as P53, mTOR, BAX, BCL2, and Caspase 3. The key pathways were apoptosis, the p53 signaling pathway, autophagy, apoptosis, the mTOR signaling pathway, dopaminergic synapses and the AMPK signaling pathway, according to the KEGG enrichment analysis (Fig. 1D). The results of GO analysis showed that the mechanism of action is mainly through the regulation of protein phosphorylation, apoptotic process, neuron apoptotic process, response to oxidative stress and other biological processes. Action on mitochondria, cytosol, cytoplasm, endoplasmic reticulum membrane and other cell components affects protein kinase activity, oxidoreductase activity, dopamine neurotransmitter receptor activity and other molecular functions (Fig. 1E).

3.2. BCT plays a role in a PD model

As shown in Fig. 2A. Compared with the NC group, the climbing time of the model group was substantially increased ($P < 0.05$). However, the climbing time in the high-dose group was considerably decreased ($P < 0.05$). Compared with the NC group, the number of autonomous activities in the model group decreased significantly ($P < 0.05$). Compared with the model group, the number of autonomous activities in the middle- and high-dose BCT groups increased significantly ($P < 0.05$).

As shown in Fig. 2B. In the NC group, the morphology of neurons in the substantia nigra region was normal, the cell structure was complete and orderly, and no obvious shrinkage occurred. However, α-syn mice showed neuronal shrinkage in the substantia nigra region, marked nucleopoiesis, unclear boundaries between nuclei and cytoplasm, and damage to neuronal structure. Although the low-dose effect was not obvious, the other two BCT treatment groups showed a small number of wrinkled neurons, and the shape was significantly improved.

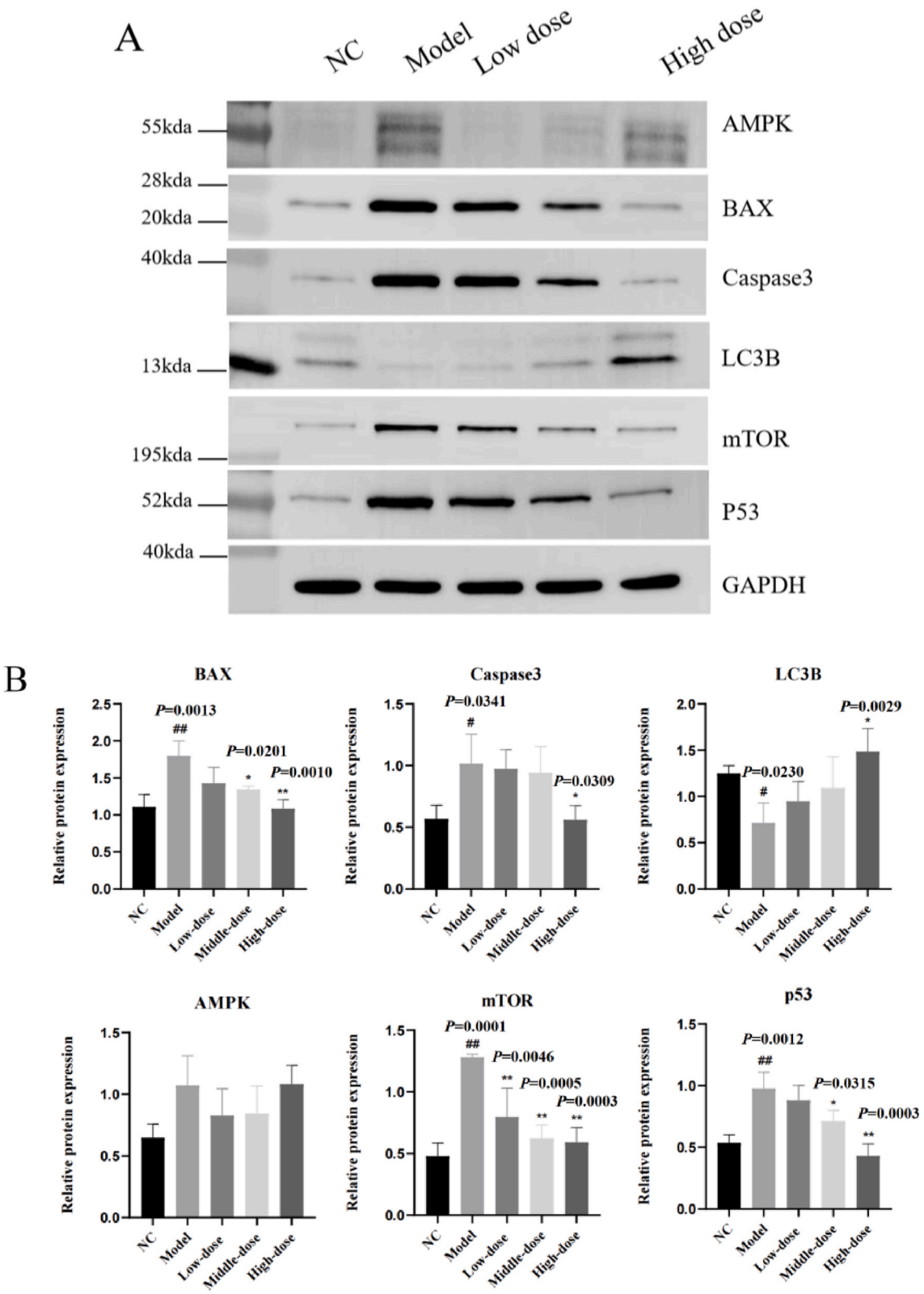

Fig. 3. (A) Western blots of AMPK,BAX,Caspase3,LC3B,mTOR and P53 in the brain tissue (refer to Fig. S1-Fig. S7). (B) Quantification of each western blotting band. Data are presented as mean with SEM, n = 3, $^{\#}P < 0.05$ and $^{\#\#}P < 0.01$ significant different from control group; $^{*}P < 0.05$ and $^{**}P < 0.01$ significant different from model group(one-way ANOVA).

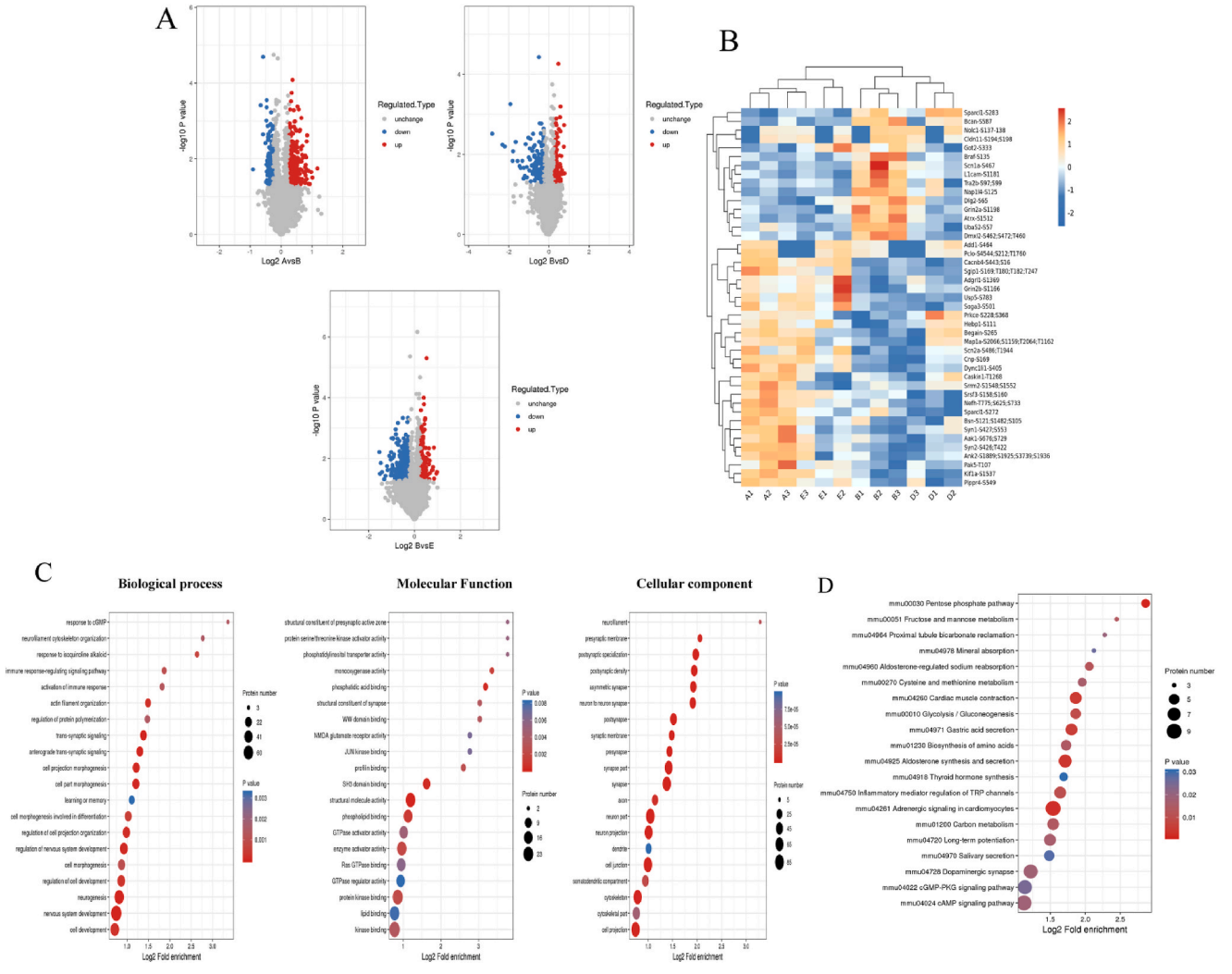

Fig. 4. (A)Volcano plot showing the differentially expressed proteins (DEPs) between groups(A:NC; B:Model; D:Middle dose; E:High dose); The horizontal axis is the value of protein Fold Change after Log_2 logarithmic conversion, and the vertical axis is the value of p-value after Log_{10} logarithmic conversion after difference significance test. Red dots represent sites with significantly up-regulated expression, and blue dots represent sites with significantly down-regulated expression. The gray dots indicate the remaining multiple change. Blue dots indicate $log_2FC < -1$ with statistical significance, and red dots indicate $log_2FC > 1$ with statistical significance.(B)Bubble chart of enrichment distribution of proteins corresponding to differentially phosphorylated modification sites in GO functional classification.(C)Bubble chart of protein KEGG enrichment distribution corresponding to different phosphorylation modification sites.

Tyrosine hydroxylase (TH) is a key enzyme in dopamine synthesis and tends to validate the successful establishment of PD models and to evaluate the severity of PD pathology. As shown in Fig. 2C, compared with the NC group, the TH level of the substantia nigra in the model group was significantly decreased ($P < 0.01$). TH levels in the substantia nigra were significantly increased in the high-dose groups ($P < 0.01$). Although there was an upward trend in the low-medium dose group, there was no statistical significance.

3.3. *Effect of BCT on the expression of p53/AMPK/mTOR signaling pathway-related proteins in the PD mouse brain*

According to the network pharmacology results, we found that apoptosis and autophagy are involved in the process of BCT treatment of PD, and disordered autophagy can lead to the release of apoptotic factors into the cytoplasm and induce apoptosis. As shown in Fig. 3A and B, C3B is the signature protein for detecting autophagy, and proper autophagy has a protective effect on cells. As an apoptosis-related factor, the upregulated expression of Bax protein can activate the downstream apoptosis signaling pathway mediated by Caspase-3 and synergistically accelerate apoptosis. Compared with those in the NC group, the Bax and Caspase-3 proteins in the α-syn mice were significantly increased ($P < 0.01$), and LC3B was significantly decreased ($P < 0.05$). Compared with the model group, the Bax and Caspase-3 protein levels in the high-dose BCT group were significantly decreased ($P < 0.05$).

It is speculated that BCT can effectively reduce the symptoms of PD mice and improve their motor function. The mechanism of action may be related to the upregulation of the autophagy level of LC3B and the timely clearance of damaged cells to protect normal cells. It also reduces the expression of the pro-apoptotic proteins Bax and Caspase-3, thereby reducing cell apoptosis and repairing nerve damage. These results indicate that autophagy factors and apoptosis factors are involved in the process of brain tissue injury in PD mice, which may be one of the mechanisms of brain tissue injury in PD mice.

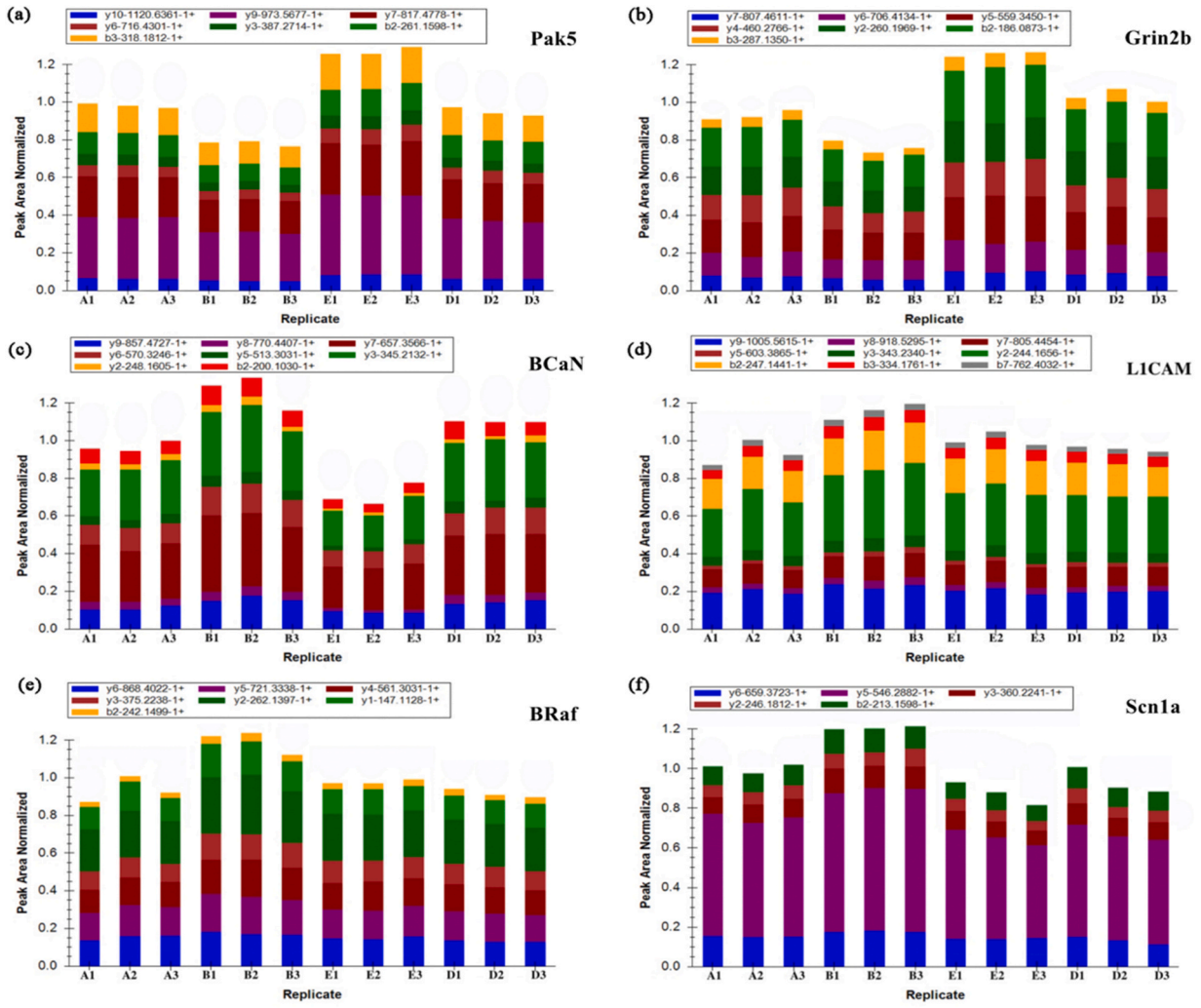

Fig. 5. Distribution of fragment ion peak area. (a) Pak5 site fragment ion peak area distribution, (b) Grin2b site fragment ion peak area distribution, (c) BCaN site fragment ion peak area distribution, (d) L1CAM site fragment ion peak area distribution, (e) BRaf site fragment ion peak area distribution, (f) Scn1a site fragment ion peak area distribution.

Furthermore, compared with the NC group, the P53 and mTOR contents of the model group were significantly increased ($P < 0.05$). The BCT group significantly downregulated P53 and mTOR levels to regulate apoptosis and autophagy but had no significant effect on AMPK. It is speculated that BCT may reduce the expression of Bax and Caspase-3 proteins through the p53/mTOR signaling pathway and inhibit cell apoptosis. The role of the p53/mTOR signaling pathway in BCT treatment of PD was further verified.

3.4. Phosphorylated proteomics data description

A total of 10,409 phosphorylated modification sites were identified on 3449 proteins, of which 9568 sites on 3245 proteins had quantitative information(Fig. S2A). In this part of the study, principal component analysis (PCA) and relative standard deviation analysis (RSD) were used to evaluate the quantitative reproducibility of the modification. As shown in the repeated sample set in the figure below, the quantitative repeatability is good, and the overall RSD value is small ($0 < RSD < 0.2$), which is qualified, indicating that the quantitative value has a good effect and good repeatability (Fig. S2BC).

We mapped the volcano map visualizing phosphorylpeptides to more graphically depict the differentially expressed proteins (Fig. 4A). The p value obtained by the T test proved the significance of the difference between groups. When the p value < 0.05, the difference modification amount change was more than 1.2 as the significantly upregulated change threshold and less than 0.833 as the significantly downregulated change threshold. Among these differentially phosphorylated protein sites, 363 significantly different phosphorylated sites were identified in the control/model group: 266 were upregulated and 97 were downregulated. In the middle/model group, 282 distinct phosphorylation sites were identified, 102 upregulated and 180 downregulated. In the high/model group, 462 distinct phosphorylation sites were identified, 188 upregulated and 274 downregulated. Since the treatment effect of the low-dose group was not obvious, the comparison will not be made here. In addition, we analyzed and compared the common differentially phosphorylated protein sites of the 4 groups, with a total of 85 phosphorylated sites (Fig. 4B).

3.5. Functional enrichment analysis of differentially expressed proteins

The comparison results between multiple groups are shown in the following figures (Fig. 5B). As shown in Fig. 4C, at the biological process level, phosphorylation sites related to nervous system development, neurogenesis, and cell projection morphogenesis were significantly enriched. At the cellular component level, phosphorylation sites related to cell projection, neuron part, neuron projection, and synapse were significantly enriched. At the molecular function level, phosphorylated proteins related to protein kinase binding, enzyme activator activity, and calmodulin binding were highly enriched and significantly different. KEGG enrichment analysis of all differentially expressed proteins revealed the following pathways: the pentose phosphate pathway, glycolysis/gluconeogenesis, cysteine and methionine metabolism, cAMP signaling pathway and cGMP-PKG signaling pathway (Fig. 4D).

3.6. PRM validation experiment

We found that Pak5, Grin2b, Scn1a, BcaN, L1cam, and Braf are closely related to network-based pharmacological screening targets and may be involved in autophagy and apoptosis pathways. The six target proteins selected above were quantified by PRM (Table 1). PRM is quantified by peak area. The distribution of fragment ion peak areas of the selected peptide segments of each protein in the samples is as follows (Fig. 5a-f). Compared with those in the NC group, the phosphorylation sites Bcan, L1CAM, Braf and Scn1a in the model group were significantly upregulated ($P < 0.05$), while Pak5 and Grin2b were significantly downregulated ($P < 0.05$). Compared with those in the model-dose group, the phosphorylation sites Pak5 and Grin2b in the middle group were significantly upregulated ($P < 0.05$), and the phosphorylation sites Bcan, L1cam, Braf and Scn1a were significantly downregulated ($P < 0.05$). In the high-dose group, the phosphorylated proteins Pak5 and Grin2b were significantly upregulated ($P < 0.05$), and Bcan, L1cam, Braf and Scn1a were significantly downregulated ($P < 0.05$).

4. Discussion

PD is a common degenerative disease of the chronic nervous system that afflicts middle-aged and elderly individuals. Its clinical symptoms are complex, but the main symptoms are decreased coordination ability and activity ability [22]. In terms of behavioral evaluation, the rotating test and rotating rod test are the conventional criteria to judge the success of PD [23]. From a behavioral point of view, the attachment ability of mice in the model group was weak, the pole climbing time was prolonged, the autonomous activity

Table 1
Quantitative results of PRM protein.

Protein Accession	Protein/Gene	A/B Ratio	B/E Ratio	B/D Ratio	B/C Ratio
K05736	PAK5	1.26	0.62	0.83	–
K05210	Grin2b	1.22	0.59	0.73	–
K04833	Scn1a	0.84	1.38	1.30	–
K04348	BcaN	0.77	1.77	1.14	–
K06550	L1CAM	0.82	1.16	1.26	–
K04365	Braf	0.79	1.20	1.28	–

was reduced, and the coordination was poor, which is consistent with the pathological behavior of PD. There was a contraction of neurons in the substantia nigra of the midbrain. BCT can significantly shorten the crawling time and increase the number of autonomous activities to improve behavioral symptoms, thus proving the effectiveness of BCT from a macro perspective. Our results showed that TH-positive expression decreased significantly in the substantia nigra of α-syn mice. TH expression can be detected to reflect the damage of dopaminergic neurons. After BCT intervention, TH content increased, indicating that BCT can inhibit or delay the loss of dopaminergic neurons, thereby improving their motor function.

Network pharmacology emphasizes analyzing the molecular correlation laws among drugs, diseases and pathways from the perspective of the system level and biological network as a whole. It is speculated that the pathways with a high correlation of the effects of BCT are apoptosis, the p53 signaling pathway, and autophagy, and the proteins with a high correlation are Bax, Caspase-3, P53, and mTOR. Western blotting and protein phosphorylation experiments verified the pathways and proteins involved in this result and clarified the correlation mechanism. It has been demonstrated that apoptosis is an important factor causing the loss of dopaminergic neurons in the substantia nigra region of the brain in PD models. Degenerative diseases such as Parkinson's disease are accompanied by autophagy defects, and the attenuation of autophagy is likely to be an important factor in the continuous apoptosis of neurons in patients with degenerative diseases [24]. Autophagy plays an important role in cell proliferation, growth, apoptosis, and maintenance of intracellular environmental homeostasis [25]. There are various signaling interactions between apoptosis and autophagy, and they are involved in the neuronal damage process [26]. Apoptosis-related caspase family proteins can interact with autophagy-related proteins. Caspase-3 inhibits autophagy-induced apoptosis by shear inactivation of Beclin-1 [27]. Mild and moderate autophagy can maintain the dynamic balance of axons and effectively remove dead cells, which is the pathway for cell survival. The protein expressed by the BCL-2-associated X protein(Bax) is dependent on the interleukin-3 (IL-3) apoptotic pathway and is an apoptosis-regulating protein. It accelerates programmed cell death by binding to inhibitors of apoptosis [28]. Our experimental results showed that the LC3B protein expression level in the substantia nigra region of mice increased significantly after BCT intervention, while Bax and Caspase-3 protein expression levels decreased significantly, suggesting that BCT may upregulate the autophagy level of LC3B and inhibit apoptosis in substantia nigra region neurons.

P53 is involved in the whole process of apoptosis and autophagy and plays an important role in regulating nutrient metabolism, DNA damage and the repair of cells [29]. When hypoxia occurs in nerve cells, the P53 protein is activated, which opens the mitochondrial membrane by regulating the BCL-2 protein, resulting in the release of Cyt-c, which further activates the caspase cascade and induces apoptosis [30]. At the same time, the activated P53 protein can upregulate the pro-apoptotic p53/AMPK pathway, which is a classical signaling pathway that regulates autophagy [31]. It has been found that p53 exists widely in the cytoplasm and nucleus and has bidirectional regulation during autophagy [32]. The P53 protein can activate the AMPK subunit to regulate cell proliferation and apoptosis. In this process, by reducing the synthesis of adenosine triphosphate, the feedback increases the content of adenosine phosphate in the cell, and the ratio of AMP/ATP increases so that the cell cannot carry out normal cycle metabolism and induces apoptosis [33]. Activation of AMPK can activate liver kinase B1, and abnormal phosphorylation of PAK protein leads to insufficient energy supply, both of which lead to the activation of mTOR protein, which directly induces an increase in intracellular phosphatidylinositol kinase activity and inhibits the initiation of autophagy [34]. In contrast, BCT was able to significantly regulate the protein expression of p53 and mTOR but had no significant effect on AMPK. These results suggest that the mechanism by which BCT inhibits apoptosis in nigrostriatal dopaminergic neurons of PD mice is related to the regulation of autophagic and apoptotic responses mediated by the p53/mTOR pathway. Therefore, these highly network-related target proteins all participate in the process of regulating apoptosis in their respective physiological activities. It was preliminarily proven that the mechanism of BCT in treating PD was to

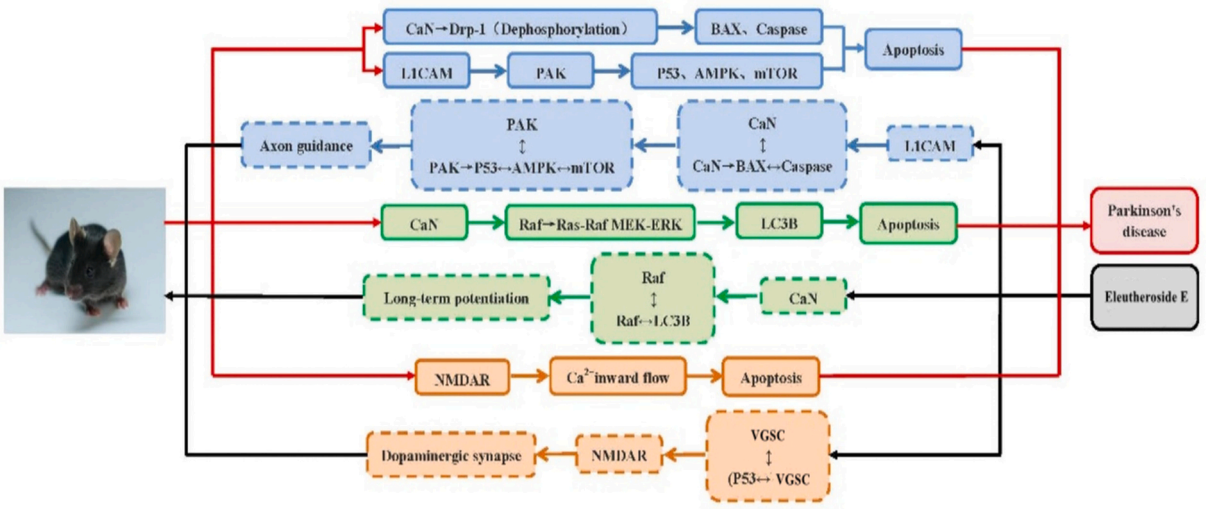

Fig. 6. Intervention of BCT on three important phosphorylation pathways. Different colors represent three pathways. The solid line box represents the pathogenesis of PD, and the dotted line box represents the mechanism of BCT in treating PD.

inhibit neuronal apoptosis. To further study the process and role relevance of these target proteins in regulating apoptosis, we next carried out protein phosphorylation detection.

Among protein modifications, phosphorylation is the most common type of protein posttranslational modification. The phosphorylation process is relatively complex, most of which is realized through the interaction between proteins, which can change the function and activity of proteins, thereby affecting the apoptosis process. To explore whether the effects of BCT on apoptosis demonstrated above are related to protein phosphorylation, phosphorylation detection of samples was performed. Using phosphorylated proteomics and PRM validation, we found that Pak5, Grin2b, Scn1a, BcaN, L1cam and Braf are closely correlated with the targets of the web-based pharmacological screen and may be involved in p53/mTOR-mediated autophagy and apoptosis pathways. This site explains the possible correlation mechanism of P53 protein, AMPK protein and mTOR protein promoting autophagy and inhibiting apoptosis in Western blot experiments (Fig. 6).

Calcineurin(CaN) is a protein phosphatase widely found in the brain that is involved in the development of many diseases such as depression and dementia, and plays an important regulatory role in neuronal excitability and synaptic plasticity [35]. Phosphorylation at the CaN site is associated with apoptosis, which induces the dephosphorylation of Drp-1 protein, which in turn leads to Bax aggregate localization and caspase protein activation, accelerating neuronal apoptosis [36]. BCT can inhibit the expression of Bax and Caspase3, and whether the inhibition of apoptosis is related to the regulation of CaN. PAK5 is a well-characterized member of the p21-activated kinases (PAKs), which impedes mitochondrial localization mainly by regulating Ser site phosphorylation [37]. It was found that PAK5 was able to reduce the activity of the apoptotic core component Caspase-3 [38]. L1 cell adhesion molecule (L1CAM) is predominantly expressed in neuronal cells and plays an important role in neuronal migration, axon growth, fasciculation and lengthening in nervous system development [39]. When the phosphorylation of L1CAM protein is abnormal, the phosphorylation of PAK protein is hindered through the NRP1→Rac pathway, and the cells are hypoxic due to abnormal mitochondrial function and insufficient energy supply, which directly or indirectly activate autophagy and apoptosis-related proteins, such as P53 protein, AMPK protein, and mTOR protein, and induce apoptosis [40,41].

Therefore, combined with phosphorylated proteomics and PRM validation, by interfering with L1CAM phosphorylation sites, BCT can affect CaN, reduce the change in CaN, and slow the dephosphorylation process, thereby preventing BAX aggregation and caspase protein activation and inhibiting neuronal apoptosis. At the same time, L1CAM affects downstream PAK, recovers mitochondrial function, and directly or indirectly inhibits P53, AMPK, mTOR and other apoptotic proteins after recovering normal phosphorylation physiological processes and then regulates the axon guidance pathway.

The Braf gene encodes a cellular signaling RAF kinase protein that activates its downstream MEK through phosphorylation. The MAPK/ERK signaling pathway can regulate cell growth, proliferation, differentiation and apoptosis [42]. The Ras/Raf/MEK/ERK signaling pathway can be activated by reactive oxygen species(ROS), Ca^{2+}, protein kinase C(PKC), etc. Inhibition of the Ras-Raf-MEK-ERK signaling pathway has an impact on cell apoptosis [43]. In recent years, the mechanism by which the Ras-Raf-MEK-ERK signaling pathway regulates autophagy has received much attention, but the mechanisms involved in the regulation of autophagy are extremely complex and sometimes seem to contradict each other [44]. Studies have shown that the Ras/Raf/MEK/ERK signaling pathway can activate ERK under stress conditions and directly promote the upregulation of the autophagy signature proteins LC3 and p62, initiating autophagy [45]. In addition, it has been confirmed that the activated Ras/Raf/MEK/ERK signaling pathway can inhibit autophagy indirectly by activating the PI3K/Akt/TOR signaling pathway [46]. In addition, SD118-xanthocillin X [1] derived from penicillin can inhibit the Ras/Raf/MEK/ERK signaling pathway in HT-29 cells, upregulate the expression levels of the autophagy marker protein LC3, and promote the occurrence of autophagy [47]. According to proteomics and its verification results, we found that BCT could downregulate the expression levels of Braf, suggesting that it could hinder the phosphorylation of RAF kinase protein, further inhibit the Ras/Raf/MEK/ERK signaling pathway, and thus upregulate the expression levels of autophagy marker protein LC3, playing a role in the positive regulation of autophagy.

N-methyl-D-aspartic acid receptor(NMDAR) is a glutamate-gated ionic glutamate receptor. The NMDAR site is a highly permeable Ca^{2+} ligand-gated ion channel complex that mediates changes in synaptic plasticity [48]. Continuous activation of NMDARs can lead to increased intracellular calcium content and metabolic enzyme activity, cytotoxicity, oxidative stress, accumulation of oxidative metabolites and loss of nitrogen ion free radicals, eventually leading to degeneration and death of nerve cells [49]. The expression activity of NMDAR in PD animal models can lead to changes in PD symptoms, and blocking the nigrostriatal reticular structure can alleviate the symptoms of PD movement disorders [50]. Glutamate-mediated excitatory neurotoxicity is closely related to the degeneration of PD, and this excitability is regulated by NMDARs. NMDAR glutamate site subunit activation and factor conversion expression can regulate glutamate release and play a certain role in mediating the neurotransmission function of glutamate in the brains of PD patients [51]. It is related to many functions of the central nervous system, and its gene variation, especially subtype gene variation, is closely related to the abnormal function of the nervous system [52]. In mammals, GRIN2B activates glutamate binding sites and dominant excitatory neurotransmitter receptors. The GRIN2B gene variant is common in Asian populations [53]. GRINB gene polymorphisms could be used as markers to evaluate PD [54]. Other researchers believe that impulsive control and related behavioral manifestations in PD patients are related to GRINB gene polymorphisms [55,56]. Our results showed that the decrease in grin2b content in the brain tissue of α-*syn*-overexpressing mice led to an increase in glutamate release regulated by NMDAR and accelerated the process of neurodegeneration. BCT can prevent Ca^{2+} inflow by increasing the content of grin2b, increasing the phosphorylation of NMDAR, blocking the influence of the nigrostriatal reticular structure, and then correcting the movement disorder symptoms of PD.

Volt-gated sodium channels (VGSCs), consisting of one pore-forming α subunit and up to two associated β subunits, play a critical role in the generation of action potentials in excitable tissues, including brain neurons [57]. Nav1.1(scn1a/SCN1A) is one of the voltage-gated sodium channel α subunits expressed in brain nerve tissue and plays a crucial role in neuronal function [58]. The loss of Nav1.1 function in mice leads to severe impairment of sodium current and action potential discharge in hippocampal GABA-inhibited

neurons [59]. Our experimental results show that the content of scn1a in PD mice is increased, and its phosphorylation causes VGSC to be turned on, causing abnormal neuron firing and causing PD behavioral symptoms.In addition, activation of the P53 protein can promote the opening of VGSCs, leading to abnormal neuronal firing. We found that BCT can regulate the activity of P53, close the VGSC channel, and prevent abnormal neuronal discharge, thus inhibiting apoptosis and protecting against neuronal damage.

5. Conclusion

In this work, network pharmacological analysis showed that the key pathways associated with BCT treatment of PD were apoptosis, the p53 signaling pathway, and autophagy. The expression levels of BAX, Caspase-3, LC3B, P53 and mTOR core proteins were further verified by western blotting. Combined with the phosphorylated proteome results, we found that Pak5, Grin2b, Scn1a, BcaN, and L1cam may be involved in p53/mtor-mediated autophagy and apoptosis pathways. It was further verified that BCT can inhibit the apoptosis of substantia nigra neurons in Parkinson's disease mice and alleviate behavioral disorders, which is related to the regulation of autophagy and apoptosis mediated by the P53/mTOR pathway. This study preliminarily clarified the molecular target and mechanism of BCT in the treatment of PD and provided a new idea for its development and application.

Data availability statement

Data associated with this study has been deposited at NCBI under the accession number PXD047887. The original contributions presented in the research are included in the article/supplementary data, and further queries can be directed to the corresponding authors.

CRediT authorship contribution statement

Xin Gao: Writing – original draft, Visualization, Methodology, Formal analysis. **Jiaqi Fu:** Software, Methodology, Formal analysis. **DongHua Yu:** Visualization, Methodology, Formal analysis. **Fang Lu:** Writing – review & editing, Validation. **Shumin Liu:** Writing – review & editing, Funding acquisition.

Declaration of competing interest

The authors declare the following financial interests/personal relationships which may be considered as potential competing interests:Shumin Liu reports financial support was provided by Heilongjiang University of Chinese Medicine. Shumin Liu reports a relationship with Heilongjiang University of Chinese Medicine that includes: funding grants. If there are other authors, they declare that they have no known competing financial interests or personal relationships that could have appeared to influence the work reported in this paper.

Acknowledgments

This work was supported by National Natural Science Foundation of China (No. 81774188),Heilongjiang Postdoctoral Program (No. ZHY2022-114),General program of Heilongjiang Province (No. LBHZ22251) and Young Elite Scientists Sponsorship Program (No. 2022-QNRC1-27)

Appendix A. Supplementary data

Supplementary data to this article can be found online at https://doi.org/10.1016/j.heliyon.2024.e26916.

References

[1] M.A. Nalls, N. Pankratz, C.M. Lill, et al., Large-scale meta-analysis of genome-wide association data identifies six new risk loci for Parkinson's disease, Nat. Genet. 46 (9) (2014) 989–993.
[2] H.M. Al-Kuraishy, A.I. Al-Gareeb, Y.H. Elewa, M.H. Zahran, A. Alexiou, M. Papadakis, G.E. Batiha, Parkinson's disease risk and hyperhomocysteinemia: the possible link, Cell. Mol. Neurobiol. (2023 Apr 19) 1–7.
[3] M. Alrouji, H.M. Al-Kuraishy, A.K. Al-Buhadily, A.I. Al-Gareeb, E. Elekhnawy, G.E. Batiha, DPP-4 inhibitors and type 2 diabetes mellitus in Parkinson's disease: a mutual relationship, Pharmacol. Rep. (3) (2023 Jun) 1–4.
[4] M. Alrouji, H.M. Al-Kuraishy, A.K. Al-Mahammadawy, A.I. Al-Gareeb, H.M. Saad, G.E. Batiha, The potential role of cholesterol in Parkinson's disease neuropathology: perpetrator or victim, Neurol. Sci. (2023 Jul 10) 1–4.
[5] G.E. Batiha, H.M. Al-Kuraishy, A.I. Al-Gareeb, E. Elekhnawy, SIRT1 pathway in Parkinson's disease: a faraway snapshot but so close, Inflammopharmacology 31 (1) (2023 Feb) 37–56.
[6] A. Atik, T. Stewart, J. Zhang, Alpha-Synuclein as a biomarker for Parkinson's disease, Brain Pathol. 26 (2016) 410–418.
[7] D.K. Verma, B.A. Seo, A. Ghosh, S.X. Ma, K. Hernandez-Quijada, J.K. Andersen, H.S. Ko, Y.H. Kim, Alpha-Synuclein preformed fibrils induce cellular senescence in Parkinson's disease models, Cells (2021) 10.
[8] M. Alrouji, H.M. Al-Kuraishy, A.I. Al-Gareeb, D. Zaafar, G.E. Batiha, Orexin pathway in Parkinson's disease: a review, Mol. Biol. Rep. (2023 May 8) 1–4.

[9] C. Alvarez-Salamero, R. Castillo-Gonzalez, G. Pastor-Fernandez, I.R. Mariblanca, J. Pino, D. Cibrian, M.N. Navarro, IL-23 signaling regulation of pro-inflammatory T-cell migration uncovered by phosphoproteomics, PLoS Biol. 18 (2020) e3000646.
[10] R. Cacabelos, Parkinson's disease: from pathogenesis to pharmacogenomics, Int. J. Mol. Sci. 18 (2017).
[11] S. Ghavami, S. Shojaei, B. Yeganeh, et al., Autophagy and apoptosis dysfunction in neurodegenerative disorders, Prog. Neurobiol. 112 (2014) 24–49.
[12] F. He, G. Qi, Q. Zhang, et al., Quantitative phosphoproteomic analysis in alpha-synuclein transgenic mice reveals the involvement of aberrant p25/Cdk5 signaling in early-stage Parkinson's disease, Cell. Mol. Neurobiol. 40 (6) (2020) 897–909.
[13] D.T. Ju, K. Sivalingam, W.W. Kuo, et al., Effect of vasicinone against paraquat-induced MAPK/p53-Mediated apoptosis via the IGF-1R/PI3K/AKT pathway in a Parkinson's disease-associated SH-SY5Y cell model, Nutrients 11 (7) (2019) 1655.
[14] H.M. Al-kuraishy, A.I. Al-Gareeb, A. Alexiou, M. Papadakis, A.A. Alsayegh, N.H. Almohmadi, H.M. Saad, G.E. Batiha, Pros and cons for statins use and risk of Parkinson's disease: an updated perspective, Pharmacology Research & Perspectives 11 (2) (2023 Apr) e01063.
[15] M. Alrouji, H.M. Al-Kuraishy, A.I. Al-Gareeb, H.M. Saad, G.E. Batiha, A story of the potential effect of non-steroidal anti-inflammatory drugs (NSAIDs) in Parkinson's disease: beneficial or detrimental effects, Inflammopharmacology 31 (2) (2023 Apr) 673–688.
[16] M. Alrouji, H.M. Al-Kuraishy, A.I. Al-Gareeb, N.A. Ashour, M.S. Jabir, W.A. Negm, G.E. Batiha, Metformin role in Parkinson's disease: a double-sword effect, Mol. Cell. Biochem. (2) (2023 Jun) 1–7.
[17] H.M. Al-Kuraishy, A.I. Al-Gareeb, A.A. Alsayegh, W.F. Abusudah, N.H. Almohmadi, O.A. Eldahshan, E.A. Ahmed, G.E. Batiha, Insights on benzodiazepines' potential in Alzheimer's disease, Life Sci. (2023 Feb 28) 121532.
[18] S. De, G. Jing, W. Ying, et al., The clinical features of autonomic dysfunction in patients with early and mid-stage Parkinson's disease and the characteristics of TCM syndrome differentiation, Shanghai J. Tradit. Chin. Med. 55 (6) (2021) 15–20.
[19] Y. Bin, Z. Lin, L. Shumin, et al., Study on the compatibility ratio of Fuyuanpingchanning compound and its anti-Parkinsonian effect, Acta Chinese Medicine and Pharmacology 34 (3) (2006) 16–18.
[20] R. Yandong, J. Yuee, Z. Shuxiang, et al., Effects of Baichanting compound on neuroinflammation in Parkinson's disease model mice, Chin. J. Inf. Tradit. Chin. Med. 22 (12) (2015) 68–71.
[21] R. Yandong, J. Yuee, Z. Shuxiang, et al., Effects of Baichananting compound on dopamine in a mouse model of Parkinson's disease, Chin. J. Integrated Tradit. West Med. 36 (1) (2016) 94–98.
[22] M. Alrouji, H.M. Al-kuraishy, A.I. Al-Gareeb, A. Alexiou, M. Papadakis, M.S. Jabir, H.M. Saad, G.E. Batiha, NF-κB/NLRP3 inflammasome axis and risk of Parkinson's disease in Type 2 diabetes mellitus: a narrative review and new perspective, J. Cell Mol. Med. ((Jul;27 (13):) (2023) 1775–1789.
[23] D.Z. Liu, J. Zhu, D.Z. Jin, L.M. Zhang, X.Q. Ji, Y. Ye, C.P. Tang, X.Z. Zhu, Behavioral recovery following sub-chronic paeoniflorin administration in the striatal 6-OHDA lesion rodent model of Parkinson's disease, J. Ethnopharmacol. 112 (2007) 327–332.
[24] B. Bahatyrevich-Kharitonik, R. Medina-Guzman, A. Flores-Cortes, et al., Cell death related proteins beyond apoptosis in the CNS, Front. Cell Dev. Biol. 9 (2021) 1–9.
[25] P. Zheng, Q. Bai, J. Feng, et al., Neonatal microglia and proteinase inhibitors-treated adult microglia improve traumatic brain injury in rats by resolving the neuroinflammation, Bioeng Transl Med 7 (1) (2022) e10249.
[26] V. Nikoletopoulou, M. Markaki, K. Palikaras, et al., Crosstalk between apoptosis, necrosis and autophagy, Biochim. Biophys. Acta 1833 (12) (2013) 3448–3459.
[27] G. Marino, M. Niso-Santano, E.H. Baehrecke, et al., Self-consumption: the interplay of autophagy and apoptosis, Nat. Rev. Mol. Cell Biol. 15 (2) (2014) 81–94.
[28] Y. Zhuo, H. Wang, L. Zou, et al., SIRT1 attenuates apoptosis of nucleus pulposus cells by targeting interactions between LC3B and fas under high-magnitude compression, Oxid. Med. Cell. Longev. 2021 (2021) 1–11.
[29] E. White, Autophagy and p53, Csh. Perspect. Med. 6 (2016) a26120.
[30] M. Motevalian, N. Tekyeh Maroof, M.H. Nematollahi, F. Khajehasani, I. Fatemi, Atorvastatin modulates the expression of aging-related genes in the brain of aging induced by D-galactose in mice. Iran, J. Basic Med. Sci. 24 (2021) 1388–1394.
[31] Y. Cha, R. Park, M. Jang, Y. Park, A. Yamamoto, W.K. Oh, E. Lee, J. Park, 6-Azauridine induces autophagy-mediated cell death via a p53- and AMPK-dependent pathway, Int. J. Mol. Sci. 22 (2021) 2947.
[32] G. D'Orazi, P53 function and dysfunction in human health and diseases, Biomolecules 13 (2023) 506.
[33] J. Yuan, H. Liu, H. Zhang, T. Wang, Q. Zheng, Z. Li, Controlled activation of TRPV1 channels on microglia to boost their autophagy for clearance of alpha-synuclein and enhance therapy of Parkinson's disease, Adv. Mater. 34 (2022) e2108435.
[34] J. Li, L. Chen, Q. Qin, D. Wang, J. Zhao, H. Gao, X. Yuan, J. Zhang, Y. Zou, Z. Mao, Y. Xiong, Z. Min, M. Yan, C. Wang, Z. Xue, Upregulated hexokinase 2 expression induces the apoptosis of dopaminergic neurons by promoting lactate production in Parkinson's disease, Neurobiol. Dis. 163 (2022) 105605.
[35] M. Naesens, D.R.J. Kuypers, M. Sarwal, Calcineurin inhibitor nephrotoxicity, Clin. J. Am. Soc. Nephrol. 4 (2009) 481–508.
[36] A. Mano, T. Tatsumi, J. Shiraishi, N. Keira, T. Nomura, M. Takeda, S. Nishikawa, S. Yamanaka, S. Matoba, M. Kobara, H. Tanaka, T. Shirayama, T. Takamatsu, Y. Nozawa, H. Matsubara, Aldosterone directly induces myocyte apoptosis through calcineurin-dependent pathways, Circulation 110 (2004) 317–323.
[37] R.E. Menard, The Role of P21-Activated Kinase in Cell Signaling, ProQuest Dissertations Publishing, 2003.
[38] T.I. Strochlic, S. Concilio, J. Viaud, R.A. Eberwine, L.E. Wong, A. Minden, B.E. Turk, M. Plomann, J.R. Peterson, Identification of neuronal substrates implicates Pak5 in synaptic vesicle trafficking, Proceedings of the National Academy of Sciences - PNAS 109 (2012) 4116–4121.
[39] J. Kim, K. Lee, D. Ahn, K. Oh, H. Yoon, Clinical significance of L1CAM expression and its biological role in the progression of oral squamous cell carcinoma, Oncol. Rep. 49 (2023) 1.
[40] B. Mrazkova, R. Dzijak, T. Imrichova, L. Kyjacova, P. Barath, P. Dzubak, D. Holub, M. Hajduch, Z. Nahacka, L. Andera, P. Holicek, P. Vasicova, O. Sapega, J. Bartek, Z. Hodny, Induction, regulation and roles of neural adhesion molecule L1CAM in cellular senescence, Aging (Albany NY) 10 (2018) 434–462.
[41] A.E. Abdelrahman, A. Salem, A.Z. Al Attar, E. Elsebai, W. Samy, M.A. Ibrahim, H.M. Ibrahim, P53, pirh2, and L1CAM as promising prognostic biomarkers of endometrial carcinoma: an immunohistochemical and genetic study, Appl. Immunohistochem. Mol. Morphol. 30 (2022) 713.
[42] A. Mazein, A. Rougny, J.R. Karr, J. Saez-Rodriguez, M. Ostaszewski, R. Schneider, Reusability and composability in process description maps: RAS-RAF-MEK-ERK signalling, Briefings Bioinf. (2021) 22.
[43] J. Liu, N. Lv, Y. Li, L. Yu, Research progress of Ras/Raf/MEK/ERK signaling pathways in Leukemia-Review, Zhongguo shi yan xue ye xue za zhi 25 (2017) 947–951.
[44] F. Chang, L.S. Steelman, J.T. Lee, J.G. Shelton, P.M. Navolanic, W.L. Blalock, R.A. Franklin, J.A. Mccubrey, Signal transduction mediated by the Ras Raf MEK ERK pathway from cytokine receptors to transcription factors: potential targeting for therapeutic intervention, Leukemia 17 (2003) 1263–1293.
[45] X. Li, A. Ma, K. Liu, Geniposide alleviates lipopolysaccharide-caused apoptosis of murine kidney podocytes by activating Ras/Raf/MEK/ERK-mediated cell autophagy, Artif. Cell Nanomed. Biotechnol. 47 (2019) 1524–1532.
[46] A. Vivek, K.M. Debarshi, K.B. Sanjay, PI3K/Akt/mTOR and Ras/Raf/MEK/ERK signaling pathways inhibitors as anticancer agents: structural and pharmacological perspectives, Eur. J. Med. Chem. 109 (2016).
[47] Y. Zhao, H. Chen, Z. Shang, B. Jiao, B. Yuan, W. Sun, B. Wang, M. Miao, C. Huang, SD118-xanthocillin X (1), a novel marine agent extracted from Penicillium commune, induces autophagy through the inhibition of the MEK/ERK pathway, Mar. Drugs 10 (2012) 1345–1359.
[48] S. Wang, L. Bian, Y. Yin, J. Guo, Targeting NMDA receptors in emotional disorders: their role in neuroprotection, Brain Sci. 12 (2022).
[49] G. Matteo, A. Carla, D. Carlo, D. Luca, B. Paola, M. Enrico, F. Diego, NMDAR encephalitis presenting as akinesia in a patient with Parkinson disease, J. Neuroimmunol. 328 (2019).
[50] G. Sitzia, I. Mantas, X. Zhang, P. Svenningsson, K. Chergui, NMDA receptors are altered in the substantia nigra pars reticulata and their blockade ameliorates motor deficits in experimental parkinsonism, Neuropharmacology 174 (2020) 108136.
[51] W. Yu, W. Yang, X. Li, X. Li, S. Yu, Alpha-synuclein oligomerization increases its effect on promoting NMDA receptor internalization, Int. J. Clin. Exp. Pathol. 12 (2019) 87–100.
[52] J.B. Amin, G.R. Moody, L.P. Wollmuth, From bedside-to-bench: what disease-associated variants are teaching us about the NMDA receptor, J. Physiol. 599 (2021) 397–416.

[53] M. He, Y. Wang, X. Zhang, L. Zhang, Exploration of the potential neuroprotective compounds targeting GluN1-GluN2B NMDA receptors, J. Biomol. Struct. Dyn. (2023).
[54] A. Hassan, M.G. Heckman, J.E. Ahlskog, Z.K. Wszolek, D.J. Serie, R.J. Uitti, J.A. van Gerpen, M.S. Okun, S. Rayaprolu, O.A. Ross, Association of Parkinson disease age of onset with DRD2 , DRD3 and GRIN2B polymorphisms, Parkinsonism Relat. Disorders 22 (2016) 102–105.
[55] J. Lee, E.K. Lee, S.S. Park, J. Lim, H.J. Kim, J.S. Kim, B.S. Jeon, Association of DRD3 and GRIN2B with impulse control and related behaviors in Parkinson's disease, Mov. Disorders 24 (2009) 1803–1810.
[56] S. Zainal Abidin, E.L. Tan, S. Chan, A. Jaafar, A.X. Lee, M.H.N. Abd Hamid, N.A. Abdul Murad, N.F. Pakarul Razy, S. Azmin, A. Ahmad Annuar, S.Y. Lim, P. Cheah, K. Ling, N. Mohamed Ibrahim, DRD and GRIN2B polymorphisms and their association with the development of impulse control behaviour among Malaysian Parkinson's disease patients, BMC Neurol. 15 (2015) 59.
[57] B.J. Martiszus, T. Tsintsadze, W. Chang, S.M. Smith, Enhanced excitability of cortical neurons in low-divalent solutions is primarily mediated by altered voltage-dependence of voltage-gated sodium channels, Elife (2021) 10.
[58] T. Yamagata, I. Ogiwara, T. Tatsukawa, T. Suzuki, Y. Otsuka, N. Imaeda, E. Mazaki, I. Inoue, N. Tokonami, Y. Hibi, S. Itohara, K. Yamakawa, Scn1a-GFP transgenic mouse revealed Nav1.1 expression in neocortical pyramidal tract projection neurons, Elife (2023) 12.
[59] J. Gedeon, J.B. Pineda-Farias, M. Gold, Role of axonal translation in the upregulation of nav1.1 following nerve injury, J. Pain 23 (2022).